European Journal of Neuroscience, Vol. 18, pp. 134–142, 2003

Role of protein kinase C family in the cerebellum-dependent adaptive learning of horizontal optokinetic response eye movements in mice

Fumihiro Shutoh,[1,5] Akira Katoh,[5] Masafumi Ohki,[1,3] Shigeyoshi Itohara,[2,5] Susumu Tonegawa[4] and Soichi Nagao[1,5]
[1]Department of Physiology, Jichi Medical School, Yakushiji 3311, Minamikawachi, Tochigi 329-0498, Japan
[2]Labaratory for Behavioural Genetics, Riken BSI, Saitama, Japan
[3]Department of Otolaryngology, Faculty of Medicine, University of Tokyo, Tokyo, Japan
[4]Center for Memory and Learning, MIT,Cambridge, MA, USA
[5]CREST, Japan Science and Technology Corporation, Saitama, Japan

Keywords: adaptation, gene knockout mouse, long-term depression, optokinetic response eye movement, protein kinase C

Abstract

Among the subtypes of the Ca^{2+}-dependent protein kinase C (PKC), which play a crucial role in long-term depression (LTD), both α and γ are expressed in the cerebellar floccular Purkinje cells. To reveal the functional differences of PKC subtypes, we examined the adaptability of ocular reflexes of PKCγ mutant mice, which show mild ataxia and normal LTD. In mutant mice, gains of the horizontal optokinetic eye response (HOKR) were reduced. Adaptation of the HOKR was not affected but its retinal slip dependency was altered in mutant mice. Sustained 1-h sinusoidal screen oscillation, which induced a relatively large amount of retinal slips in both mutant and wild-type mice, increased the HOKR gain in wild-type mice but not in mutant mice. In contrast, exposure to 1 h of sustained slower screen oscillations, which induced relatively small retinal slips in mutant and wild-type mice, increased the HOKR gain in both mutant and wild-type mice. Adaptation of the HOKR of the mutant mice to slow screen oscillation and those of wild-type mice to fast and slow screen oscillations were all abolished by local applications of a PKC inhibitor (chelerythrine) within the flocculi. Electrophysiological and anatomical studies showed no appreciable changes in the sources and magnitudes of climbing fibre inputs, which mediate retinal slip signals to the flocculus in the mutant mice. These results suggest that PKCγ has a modulatory role in determining retinal slip dependency, and other PKC subtypes, e.g. PKCα, may play a crucial role in the adaptation of the HOKR.

Introduction

Protein kinase C (PKC), abundantly expressed widely in the central nervous system (CNS), contains seven subtypes (Hidaka *et al*., 1988; Nishizuka, 1988, 1992; see also Tanaka & Nishizuka, 1994) whose specific functional role is unknown. Of the seven subtypes of PKC, α, β and γ are activated in both Ca^{2+}- and diacylglycerol-dependent manner, and the other subtypes (δ, ε, η and θ) are activated in Ca^{2+}-independent manner (Shinomura *et al*., 1991; Nishizuka, 1992). Among the three Ca^{2+}-dependent PKC subtypes, γ is expressed abundantly in the cerebellar Purkinje cells and hippocampal pyramidal cells, but rarely expressed in other CNS neurons. In contrast, α is expressed in most of the CNS neurons. Activation of the Ca^{2+}-dependent PKC is necessary for induction of long-term depression (LTD) of parallel fibre-Purkinje cell synapses, which underlies cerebellar motor learning (e.g. Ito, 1989, 2001; Daniel *et al*., 1998). Activation of PKC induced LTD in cerebellar slices (Crépel & Krupa, 1988). Application of PKC inhibitors to cerebellar culture or slices blocked LTD (Linden & Connor, 1991, 1995; Linden *et al*., 1992; Chen *et al*., 1995). However, studies of gene-manipulated mice showed rather different results. Mice lacking PKCγ showed normal LTD, normal eye blink conditioning and impaired elimination of multiple climbing fibre – Purkinje cell innervations (Chen *et al*., 1995; Kano *et al*., 1995; see also Chen & Tonegawa, 1977). On the other hand, transgenic mice expressing a PKC inhibitor specifically on the cerebellar neurons showed impaired LTD, loss of adaptation of ocular reflex and impaired elimination of multiple climbing fibre – Purkinje cell innervations (De Zeeuw *et al*., 1998; Goossens *et al*., 2001). In this study, we examined the role of the PKC subtypes by analysing the cerebellum-dependent adaptation of the horizontal optokinetic response (HOKR) eye movements of PKCγ mutant mice combined with pharmacological methods. Using immunohistochemical methods we examined the location of Ca^{2+}-dependent PKC subtypes within the cerebellar flocculus, which is the essential site for the adaptation of the HOKR (Katoh *et al*., 1998). We also examined HOKR-related neural circuitry formation around the flocculus both anatomically and electrophysiologically in the mutant mice. The results suggest that the Ca^{2+}-dependent PKC subtypes may play different roles in cerebellar motor learning. Parts of the present results have been published in abstract form (Shutoh *et al*., 2001).

Materials and methods

Animals

Mice lacking PKCγ were generated as described previously (Abeliovich *et al*., 1993; Chen *et al*., 1995). PKCγ mutant and wild-type mice were 3- to 4-month-old littermates obtained by intercrossing

Correspondence: Dr S. Nagao, [1]Jichi Medical School, as above.
E-mail: nagaos@jichi.ac.jp

Received 28 January 2003, revised 1 April 2003, accepted 22 April 2003

doi:10.1046/j.1460-9568.2003.02717.x

heterozygotes that have been backcrossed to an inbred C57BL/6 mouse (Clea Japan, Tokyo, Japan) for 12 generations. Twenty-two each of PKCγ mutant and wild-type littermates were used in the examination of eye movements. The primers used for PCR-aided genotyping were 5′-GGATGACGATGTAGACTGCA-3′ and 5′-TCTGAAAGGTGGAG-TGAAGC-3′ for the wild-type allele, and 5′-TCCTGCCGAGAAAG-TATCCA-3′ and 5′-GTCAAGAAGGCGATAGAAGG-3′ for the mutant allele (neo gene cassette). PCR cycles were run at 96 °C for 30 s, 60 °C for 30 s and 72 °C for 90 s for a total of 35 cycles.

Eye movement recordings

Under pentobarbital anaesthesia (Nacalai Tesque, Kyoto, Japan; 60 mg/kg body weight) and aseptic conditions, a platform for head fixation was made on the cranial bone using four small screws and one long bolt by synthetic resin. Small holes were made on the cranial bones over the parafloccular lobe bilaterally. Usually, the mice adapted to head fixation within a few minutes. They then sat quietly in their chamber for 1 h. The experimental methods were approved by the management committee of Jichi Medical Laboratory of Experimental Medicine and followed all ethical guidelines of the principals of laboratory animal care (NIH, publication number 86-23, 1978).

Two days after surgery, the mouse was mounted on the turntable surrounded by a checked-pattern screen (screen diameter, 64 cm; screen height, 70 cm), with the head fixed and the body loosely restrained in a plastic cylinder. Eye movements were recorded with an infrared TV camera for real-time recording (Nagao, 1990; Katoh *et al*., 1998; Shutoh *et al*., 2002). The frontal view of the right eye was monitored using an infrared charge coupled device (pixel size, 768 × 494) TV camera (SSC-M350; Sony, Tokyo, Japan) through a cold mirror. The pupil of the right eye was illuminated by an infrared-light (wavelength, 900 nm)-emitting diode and displayed on a 12-inch TV monitor (magnification, 55×). The area of the pupil was determined based on the difference in brightness between the pupil and the iris. The real-time position of the eye was measured by calculating the central position of the left and right margins of the pupil at 50 Hz using a position-analysing system (C-1170; Hamamatsu Photonics, Hamamatsu, Japan) and stored in a personal computer. The mean effective diameter of the mouse eyeball was estimated to be 2.3 mm (Stahl *et al*., 2000; Shutoh *et al*., 2002). The spatial resolution of the TV camera system was 0.25°. The HOKR was tested by sinusoidal oscillation of the checked-pattern screen (screen height, 60 cm from the eye of mouse; check size, 4° or 8°) by 5–20° (peak-to-peak) at 0.11–0.17 Hz (maximum screen velocity, 2.6–10.5°/s) in light. The horizontal vestibulo-ocular reflex (HVOR) was tested by sinusoidal oscillation of the turntable in the horizontal plane by 10° (peak-to-peak) at 0.11–0.5 Hz in darkness. More than 10 cycles of the evoked eye movements free from artefacts due to blinks and saccades were averaged, and the mean amplitude and phase were calculated by a modified Fourier analysis (Jastreboff, 1979). The gain of the eye movement was defined as the ratio of the peak-to-peak amplitude of eye movements to that of the screen or turntable oscillation. The phase was defined as 0° when the peak of the eye movements matched the screen oscillation in the HOKR, and when the peak of the eye movement was opposite to the peak of turntable oscillation in the HVOR. The adaptabilities of the HOKR were examined by exposing the mouse to 1 h of sustained screen oscillation at 15° and 0.17 Hz (maximum screen velocity, 7.9°/s), and at 10° and 0.11 Hz (maximum screen velocity, 3.5°/s) in light. The HOKR was measured at 30-min intervals.

Local applications of PKCγ inhibitor

Effects of PKC inhibitors on the adaptability of the HOKR were examined as follows. First, 0.2 μL of saline was injected into the bilateral flocculi with two microsyringes (80135, Hamilton, Reno, NV, USA) mounted on standard micromanipulaters for 30 min. Thirty minutes after injection, adaptability of the HOKR was tested by 1 h of sustained sinusoidal screen oscillation (15°−0.17 Hz and 10°−0.11 Hz for wild-type mice and 10°−0.11 Hz for mutant mice). Two days later, the adaptability of the HOKR was tested for the same mouse after bilateral floccular injection of 0.5 μL of 5 mg/mL chelerythrine hydrochloride (Sigma-Aldrich, St Louis, MO, USA) dissolved in distilled water, in a manner similar to injections of saline. Finally, 3 days later, recovery of the adaptability of the HOKR of the mouse was evaluated by 1 h of sustained sinusoidal screen oscillation.

Immunohistochemistry and immunoblots

Under deep anaesthesia, six mutant and six wild-type mice were perfused with 100 mL of saline, followed by 100 mL of 4% paraformaldehyde in phosphate buffer (PB; 0.1 M, pH 7.4). Brains and eyeballs were removed and post-fixed in the same fixative for 2 h at 4 °C, and placed in a cryoprotectant solution (0.1 M PB, pH 7.4, containing 25% sucrose) for 3 days. The tissues were embedded in gelatin and then cut into 50-μm-thick coronal sections with a cryostat. These were then washed in phosphate-buffered saline (PBS, pH 7,4) three times, and pre-incubated for 1 h at room temperature with 5% normal goat serum (NGS) in PBS. The sections were then incubated with primary antibodies against each of the PKC subunits (Sigma-Aldrich) diluted as follows (α, 1 : 2000; β_1, 1 : 1000; β_2, 1 : 250 and γ, 1 : 250) in 1% NGS in PBS for 3 h at room temperature. Subsequently, the sections were rinsed in PBS and incubated for 1 h with biotinylated antirabbit IgG (Vector Laboratories, Burlingame, CA, USA) diluted 1 : 400 in 1% NGS for 1 h, and rinsed again in PBS, and incubated for an additional 1 h in an avidin–biotin–peroxidase solution (ABC-Elite; Vector Laboratories) diluted at 1 : 100 in PBS. They were then washed in PBS, and incubated in a solution containing 0.025% 3,3′-diaminobenzide tetrahydrochloride (DAB; Dojindo, Kumamoto, Japan) and 0.006% H_2O_2 for 10 min. These sections were repeatedly washed in PBS, mounted onto gelatin-coated slides, and later examined using a Leica Q500IW microscope system.

The presence of PKCγ in neural tissues was also examined by the immunoblot assay. Homogenized whole-tissue samples of the cerebellum, midbrain and eyeball were used for the immunoblot assays probed with specific antibodies against PKCγ (Sigma-Aldrich). Proteins in homogenized samples were separated by 10% sodium dodecyl sulphate polyacrylamide gel electrophoresis (SDS-PAGE) and electrophoretically transferred to membranes. The membranes were incubated with the specific antibodies for 2 h at room temperature, blocked with 10% non-fat dried milk in PBS. Immunoreactive bands were visualized by staining with BCIP (5-bromo-4-chloro-3-indolyl phosphate, Sigma-Aldrich) – NBT (nitro blue tetrazolium, Sigma-Aldrich) solution with alkaline-phosphatase antirabbit IgG (Vector Laboratories).

Neuronal labelling

Seven mutant and seven wild-type mice were used. Under pentobarbital anaesthesia, we injected either 0.5 μL of 3% fast blue (Sigma) or 0.2 μL of 15% biotinylated dextran (BD; Molecular Probes, Eugene, OR, USA) dissolved in 0.05 M Tris-HCl-buffered saline (TBS, pH 7.4) into the flocculus using a microsyringe with the needle tip covered with a glass micropipette (tip diameter, 20–30 μm) attached to a standard micromanipulator. Seven days after the injection, the mice were again deeply anaesthetized with sodium pentobarbital, and perfused with 100 mL of saline, followed by 100 mL of a fixative composed of 4% paraformaldehyde in 0.1 M PBS (pH 7.4). Brains were removed and post-fixed in the same fixative for 2 h at 4 °C, and placed in a cryoprotectant solution for 3 days. The tissues were embedded in

gelatin and then cut into 50-μm-thick coronal sections with a cryostat. For BD sections, after washing in PBS, sections were incubated with ABC-Elite solution (Vector Laboratories) for 1 h, and in a solution containing DAB (Dojindo) and 0.006% H_2O_2 for 10 min. These sections were repeatedly washed in PBS and mounted onto gelatin-coated slides. For the cerebellum and brain stem, the nomenclature of Franklin & Paxinos (1997) was followed.

Electrophysiology

Recording of extracellular field potentials was carried out in seven mutant and seven wild-type mice. Under anaesthesia with xylazine (Selactar, Bayer Yakuhin, Tokyo, Japan; 5 mg/kg body weight) and ketamine (Ketalar, Sankyo, Tokyo, Japan; 5 mg/kg body weight), a small hole was made on the bone over the right paraflocculus of mice in aseptic conditions. A glass microelectrode containing 2 M NaCl solution (resistance, 0.5–1 MΩ) was inserted into the right paraflocculus–flocculus complex. A flash of light was delivered to the right eye by a stroboscopic stimulus apparatus (SLS-3100, Nihonkohden, Tokyo, Japan) at 0.25 Hz. Evoked field potentials were recorded using standard microelectrode amplifiers (MEG-1200 and MEZ7200, Nihonkohden). Evoked respo- nses to 32 stroboscopic stimuli were averaged on a personal computer (LC-630, Apple) equipped with the Powerlab interface (PowerLab-2e, Analog Digital Instruments, New South Wales, Australia).

Effects of microstimulation of the flocculus were examined in six mutant and six wild-type mice. A small hole and head-fixing platform were made as described above under general anaesthesia. In order to observe the effects of local stimulation, a glass microelectrode was inserted to the flocculus–paraflocculus complex after the mice completely recovered from anaesthesia. Negative train pulses (frequency, 333 Hz; width, 0.15 ms; strength, <50 μA; pulse number, 40; train frequency, 0.25 Hz) were delivered via the microelectrode. Evoked eye movements were observed using the TV camera system.

The significance of the data was evaluated using a standard statistics package (Statview, version 5, SAS Institute, NC, USA). These experimental protocols followed the principles of laboratory animal care (NIH publication no. 86-23, 1978) and were approved by the management committee of Jichi Medical Laboratory of Experimental Medicine.

Results

Dynamic characteristics of reflex eye movements of PKCγ mutant mice

All the PKCγ mutant mice showed ataxic limb movements as reported previously (Chen *et al.*, 1995). Nystagmic-like small eye movements time-locked to the sporadically evoked ataxic limb movements were seen on the TV monitor. Although slight upward shifts of the spontaneous eye position were recognized both under dark ($3.7 \pm 1.1^\circ$, $n = 9$; mean ± SEM) and light ($5.8 \pm 1.0^\circ$) conditions, dynamic characteristics of the HOKR and HVOR could be evaluated in all the 22 mutant mice used. As shown in Fig. 1A, gains of the HOKR of the mutant mice were lower than those of the wild-type mice at all the parameters of screen oscillations examined ($P < 0.01$, ANOVA for multiple measurements), whereas phases of the HOKR were not different from those of wild-type mice ($P > 0.1$, ANOVA; Fig. 1C). In contrast, no significant difference was found between mutant and wild-type mice in gains or phases of the HVOR (Fig. 1B and D). The HOKR gains for 4° checked-pattern screen and those for 8° checked-pattern screen oscillations were compared in mutant and wild-type mice (Fig. 1E and F). The larger checked-pattern screen significantly decreased the gains of the HOKR irrespective of the screen velocity in both mutant and wild-type mice. The HOKR gain dependency on the check-pattern size seems to be preserved in mutant mice.

Adaptation of the HOKR in mutant mice

Sustained exposure to sufficient amounts of retinal slips for 1 h induces adaptation of the HOKR gain in mice (Katoh *et al.*, 2000). The maximum retinal slip velocity during sustained screen oscillation was estimated as the (maximum screen velocity) × $\sqrt{(1 - 2G\cos\theta + G^2)}$, where G is the mean HOKR gain and θ the mean HOKR phase (Katoh *et al.*, 2000). Adaptation of the HOKR was tested by exposing mice to $10^\circ-0.11$ Hz (Fig. 2A–D, Table 1), $10^\circ-0.17$ Hz (Table 1) and $15^\circ-0.17$ Hz (Fig. 2E–H) screen oscillations. The magnitude of retinal slips during these screen oscillations varied in mutant and wild-type mice (Table 1). The wild-type mice showed an adaptive HOKR gain increase of 0.07 ± 0.03 at conditions of $10^\circ-0.11$ Hz (Fig. 2B and D), 0.13 ± 0.02 at $10^\circ-0.17$ Hz ($n = 10$, Table 1) and 0.12 ± 0.02 at $15^\circ-0.17$ Hz (Fig. 2F and G) screen oscillations. However, the mutant mice showed an adaptive HOKR gain increase of 0.07 ± 0.03 only at the condition of $10^\circ-0.11$ Hz screen oscillation (Fig. 2A and D), which induced relatively small retinal slips (2.6°/s). No adaptive HOKR gain increase was seen in the HOKR gain at conditions of $10^\circ-0.17$ Hz ($n = 6$, Table 1) or $15^\circ-0.17$ Hz screen oscillations (Fig. 2E and H), which induced relatively large retinal slips (3.6 and 6.0°/s respectively, Table 1). Thus, the PKCγ mutant mice showed HOKR adaptation only to fairly small retinal slips. These results suggest that the knockout of PKCγ did not depress the adaptation of the HOKR, but altered its retinal slip dependency.

Effects of PKC inhibitor on the HOKR adaptation

PKC is known to play a key role in the cerebellar LTD (e.g. Ito, 2001), which is considered to underlie the adaptation of the HOKR (Katoh *et al.*, 2000; Shutoh *et al.*, 2002). We examined the effects of a subtype non-specific PKC inhibitor on the adaptation of the HOKR of the PKCγ mutant and of wild-type mice (Fig. 3). We applied water-soluble low-molecular-weight (MW, 380) chelerythrine hydrochloride (200 μM; Herbert *et al.*, 1990) or control saline into the flocculi bilaterally 30 min before the test of HOKR adaptation, as shown in Fig. 3K. Application of chelerythrine or saline had little affect on the HOKR gains (Fig. 3J). When 0.5 μL of saline was applied to the mutant mice as a control, 1 h of $10^\circ-0.11$ Hz screen oscillation induced an adaptive increase in the HOKR gain (0.05 ± 0.01, $n = 7$; Fig. 3A and C). However, when the same mice were tested with 0.5 μL of chelerythrine 3 days later, adaptation of the HOKR to 1 h of $10^\circ-0.11$ Hz screen oscillation was completely blocked (Fig. 3B and C). Four days later, the same mice were tested again to 1 h of $10^\circ-0.11$ Hz screen oscillation with no drug application, and we found that the adaptation of the HOKR recovered (Fig. 3C). Thus, the PKC inhibitor blocked the adaptation of the HOKR in PKCγ mutant mice.

Effects of the PKC inhibitor on adaptation of the HOKR were also determined in wild-type mice. When control saline was injected, the HOKR gain increased by 0.08 ± 0.03 ($n = 7$) for 1 h of sustained $10^\circ-0.11$ Hz screen oscillation (Fig. 3D and F), and 0.06 ± 0.02 ($n = 7$) for 1 h of sustained $15^\circ-0.17$ Hz screen oscillation (Fig. 3G and I). On the other hand, when 0.5 μL of chelerythrine was applied, adaptations of the HOKR to $10^\circ-0.11$ Hz screen oscillation (Fig. 3E and F) and $15^\circ-0.17$ Hz screen oscillation (Fig. 3H and I) were blocked. Four days later, the same group of mice was tested again, and we found that adaptations of the HOKR recovered (Fig. 3F and I). The application of chelerythrine abolished these adaptations of the HOKR to both small ($10^\circ-0.11$ Hz) and large ($15^\circ-0.17$ Hz) slips in wild-type mice. Thus, chelerythrine blocked HOKR adaptations of

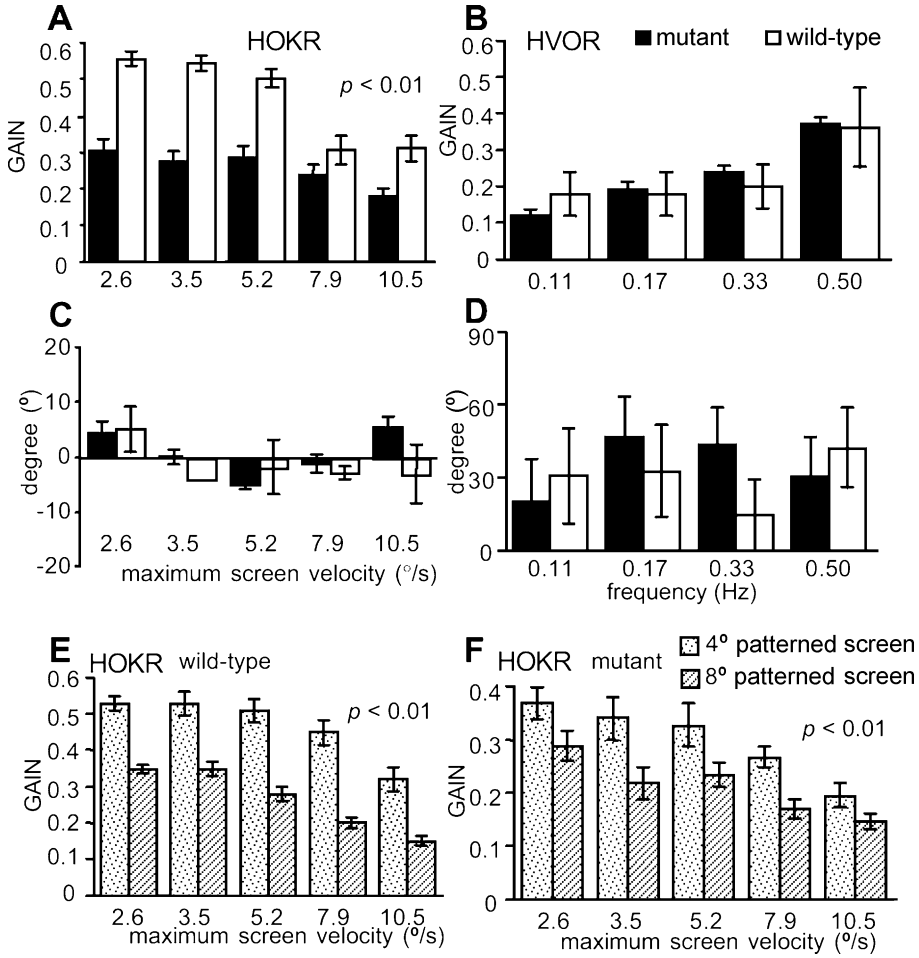

FIG. 1. Dynamic characteristics of horizontal optokinetic response (HOKR; gain, A; phase, C) and vestibulo-ocular reflex (HVOR; gain, B; phase, D) of PKCγ mutant (black columns) and wild-type (white columns) mice. HOKR was measured by sinusoidal screen oscillation of the checked-pattern (check size, 4°) screen at 5° (peak-to-peak) and 0.17 Hz (maximum screen velocity, 2.6°/s), 10° and 0.11 Hz (3.5°/s), 10° and 0.17 Hz (5.2°/s), 15° and 0.17 Hz (7.9°/s), and at 20° and 0.17 Hz (10.5°/s). Gains of the HOKR of 22 mutant mice were lower than those of 22 wild-type mice, but no difference was found in HVOR gains between mutant and wild-type mice. In E and F, HOKR gains in response to small (4°, dotted columns) or large (8°, striped columns) checked pattern screen were compared in seven mutant and seven wild-type mice. Note that gains of the HOKR were dependent on the check size of the screen in both the mutant and the wild-type mice. Statistical significance was evaluated by ANOVA for multiple measurements, and *P* values are shown in each frame. Error bars indicate standard error of the mean (SEM).

both PKCγ mutant and wild-type mice. PKC seems to play an essential role in the adaptation of the HOKR.

PKC expression within flocculus

We then examined the pattern of expression of Ca^{2+}-dependent PKC subtypes on the cerebellar flocculus Purkinje cells. As shown in Fig. 4A and E, PKCα was expressed in the flocculus Purkinje cell somata and dendrites of both mutant and wild-type mice. No clear difference was seen in PKCα staining density between mutant and wild-type flocculus Purkinje cells in our histological examination. $PKC\beta_1$ and $PKC\beta_2$ were not expressed in the Purkinje cell somata or dendrites of wild-type or mutant mice (Fig. 4B, C, F and G), although $PKC\beta_1$-positive Purkinje cells were seen (data not shown) in the vermis of both mutant and wild-type mice, as reported by Hirono *et al*. (2001). A small number of $PKC\beta_2$-positive grains were seen in the granule cell layers of the cerebellum in both mutant and wild-type mice (data not shown), as previously reported (Wetsel *et al*., 1992). PKCγ was expressed in Purkinje cell somata and dendrites of wild-type mice but not in those of mutant mice (Fig. 4D and H). We examined the expression of the PKCγ in eye-movement-related brain stem/midbrain areas and retina by immunohistochemical staining and immunoblotting using specific antibodies against PKCγ. However, no labelled neurons or immunoreactive bands were detected in these areas in adult wild-type mice (data not shown). In contrast, PKCα-specific immunoreactive bands were recognized for homogenates obtained from retina and those from the brainstem areas of both mutant and wild-type mice (data not shown).

Input and output characteristics of flocculus Purkinje cells of PKCγ mutant mice

Climbing fibre inputs to the flocculus mediate retinal slip signals necessary for induction of HOKR adaptation (e.g. Ito, 1984). Because the PKCγ mutant mice showed changes of retinal slip dependency in the adaptation of the HOKR, it is suggested that climbing fibre inputs to the flocculus are altered in mutant mice. To examine this possibility, we compared the strength of the climbing-fibre-mediated visual responses (Maekawa & Simpson, 1973) in the flocculus between the mutant and wild-type mice. Stroboscopic stimuli induced positive or negative field potentials at a latency of 10–15 ms. As shown in Fig. 5A and B, profiles of visual responses examined at 200-μm

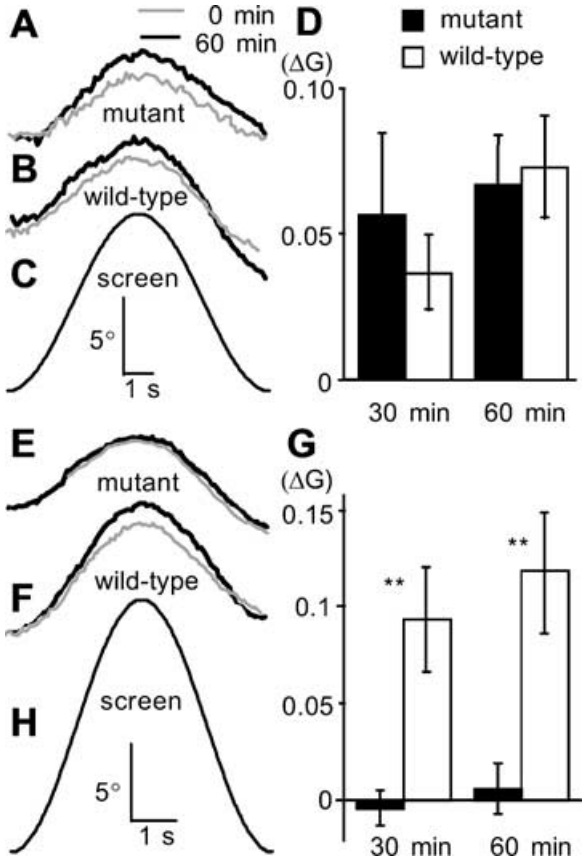

FIG. 2. Retinal slip dependency of the HOKR adaptation in mutant mice. A–D, adaptation of the HOKR for 1 h of 10°−0.11 Hz screen oscillation, which induced relatively small retinal slips. A and B show examples of averaged eye position traces obtained before (0 min) and after (60 min) 1 h of sustained screen oscillation in mutant (A) and wild-type mice (B). More than 10 eye position traces were averaged. C shows the screen position. D, HOKR gain changes during sustained screen oscillation in mutant ($n = 6$, black columns) and wild-type mice ($n = 10$, white columns). E–H, similar to A–D but for the adaptation of the HOKR by screen oscillation at 10°−0.17 Hz, which induced a large amount of retinal slips. Data in H were obtained from seven mutant and 10 wild-type mice. Error bars indicate SEM (Welch's *T*-test). $^{**}P < 0.01$.

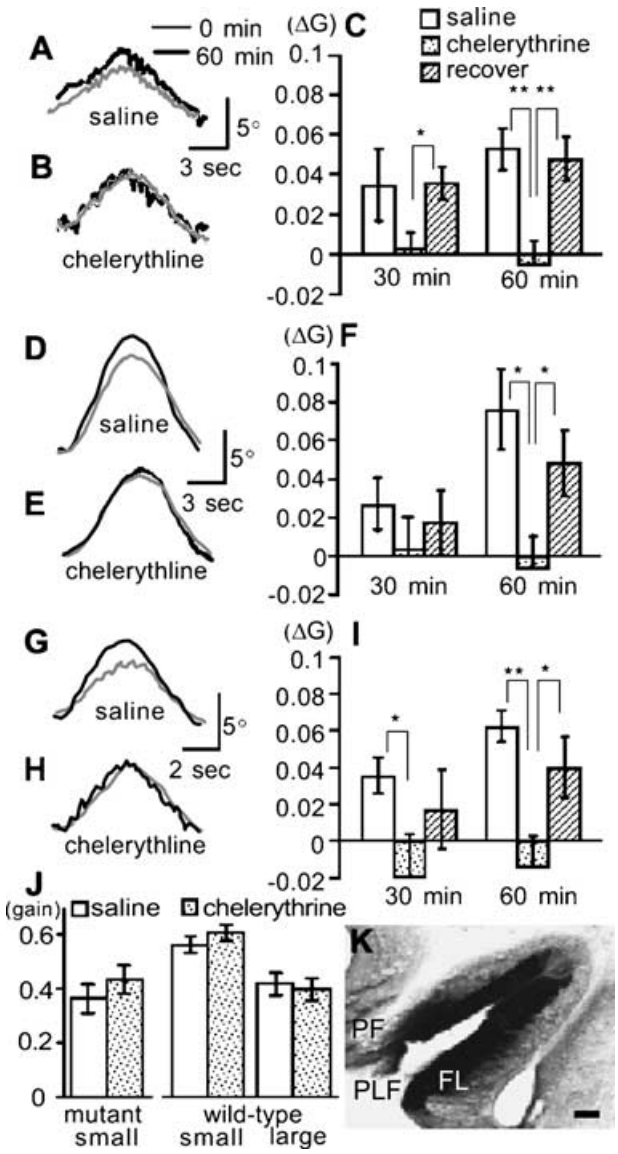

FIG. 3. Effects of PKC inhibitor on the HOKR adaptation in PKCγ mutant (A–C) and wild-type mice (D–I). Adaptation of HOKR was induced by 10°−0.11 Hz screen oscillation in mutant mice (A–C), 10°−0.11 Hz (D–F) and 15°−0.17 Hz (G–I) screen oscillations in wild-type mice. A and B show examples of averaged eye movement traces obtained from more than 10 cycles of screen oscillation at 0 min and 60 min of sustained screen oscillation after local saline (A) or chelerythrine (B) application to bilateral flocculi. C shows HOKR gain changes (mean ± SEM) during 1 h of sustained screen oscillation after saline or chelerythrine applications, and during the recovery test ($n = 7$). D–F, similar to A–C but for seven wild-type mice during 10°−0.11 Hz screen oscillation, which induced a small amount of retinal slips. G–I, similar to D–F but for 15°−0.17 Hz screen oscillation, which induced large retinal slips. J, HOKR gain at 0 min during 10°−0.11 Hz sustained screen oscillation in mutant mice, and 10°−0.11 Hz and 15°−0.17 Hz screen oscillations in wild-type mice. Note that chelerythrine injections did not affect the gains of HOKR in both mutant and wild-type mice. In K, diffusion of drug was estimated by mixed injection of chelerythrine and biotinylated dextran (BD). BD was histochemically visualized by staining with DAB. Note that BD diffused widely within the flocculus and adjacent ventral paraflocculus. Statistical significance was evaluated using Welch's *t*-test (C, F and I) or ANOVA for multiple measurements (J), $^{*}P < 0.05$; $^{**}P < 0.01$. FL, flocculus; PF, paraflocculus; PLF, postero-lateral fissure. Scale bar, 100 μm.

intervals were similar between the mutant and wild-type mice. The typical positive field potentials were observed at 500–600 μm from the surface of the paraflocculus lobe in both mutant and wild-type mice (Fig. 5B). Histological analysis revealed that the proximal one-third of molecular layer of the flocculus is located 600–800 μm from the surface of the paraflocculus (not shown). We also compared the strength of the flocculus Purkinje cell outputs between the mutant and wild-type mice because it is known that a decrease in climbing

TABLE 1. Magnitude of retinal slips during sustained screen oscillation

Maximum screen velocity (°/s)	HOKR		Maximum retinal slip velocity (°/s)	Adaptation induction
	Gain	Phase (°)		
PKCγ mutant				
3.5	0.27 ± 0.03	0.1 ± 7.6	2.6 ± 0.1	Yes
5.2	0.28 ± 0.03	−4.9 ± 6.8	3.6 ± 0.2	No
7.9	0.24 ± 0.03	−1.2 ± 2.7	6.0 ± 0.2	No
Wild-type				
3.5	0.54 ± 0.02	−4.2 ± 1.4	1.6 ± 0.1	Yes
7.9	0.30 ± 0.04	−3.0 ± 1.6	5.5 ± 0.3	Yes
5.2	0.50 ± 0.03	−1.8 ± 1.1	2.6 ± 0.2	Yes

The maximum retinal slip velocity during sustained screen oscillation was estimated as the (maximum screen velocity) × $\sqrt{(1 - 2G\cos\theta + G^2)}$, where G is the mean HOKR gain and θ the mean HOKR phase before sustained screen oscillation.

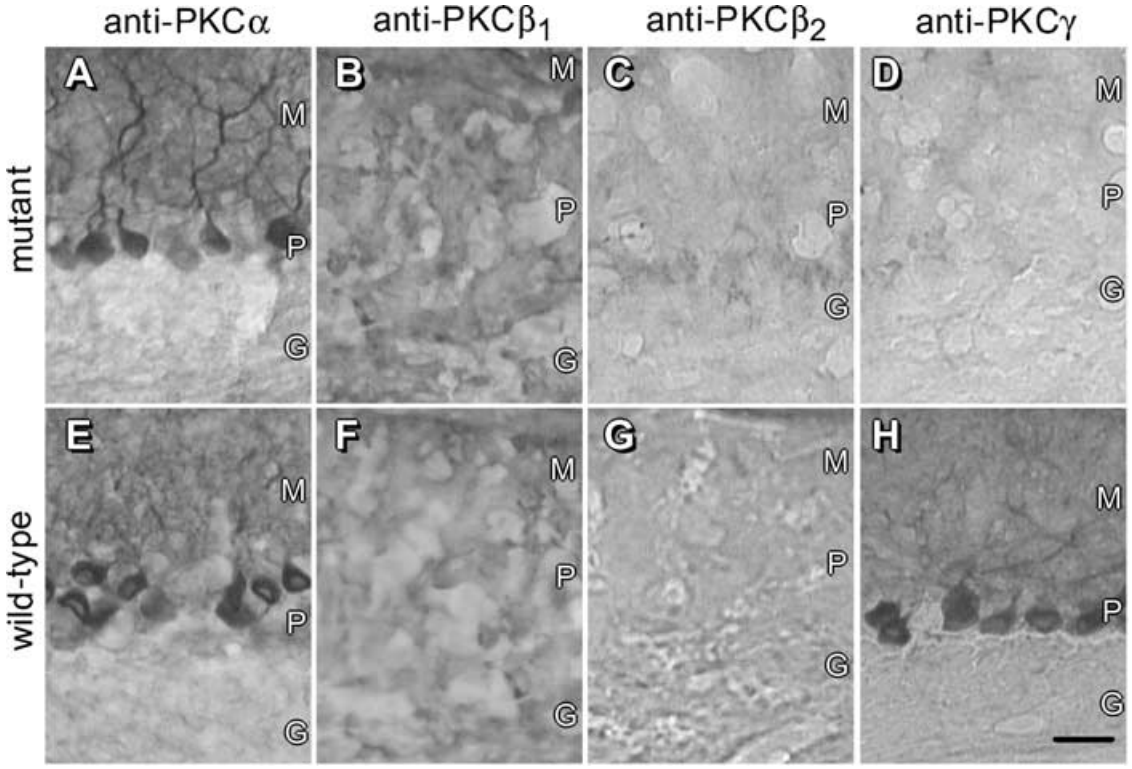

FIG. 4. Immunohistochemical staining for isozymes of Ca^{2+}-dependent PKC family in the flocculus of mutant and wild-type mice. PKCα-positive Purkinje cells were seen in both mutant and wild-type mice (A and E). PKCβ_1- or β_2-positive Purkinje cells were not seen in mutant (B and C) or wild-type (F and G) mice. PKCγ-positive Purkinje cells were seen in wild-type mice (H) but not in mutant mice (D). G, granular cell layer; M, molecular layer; P, Purkinje cell layer. Scale bar, 50 μm.

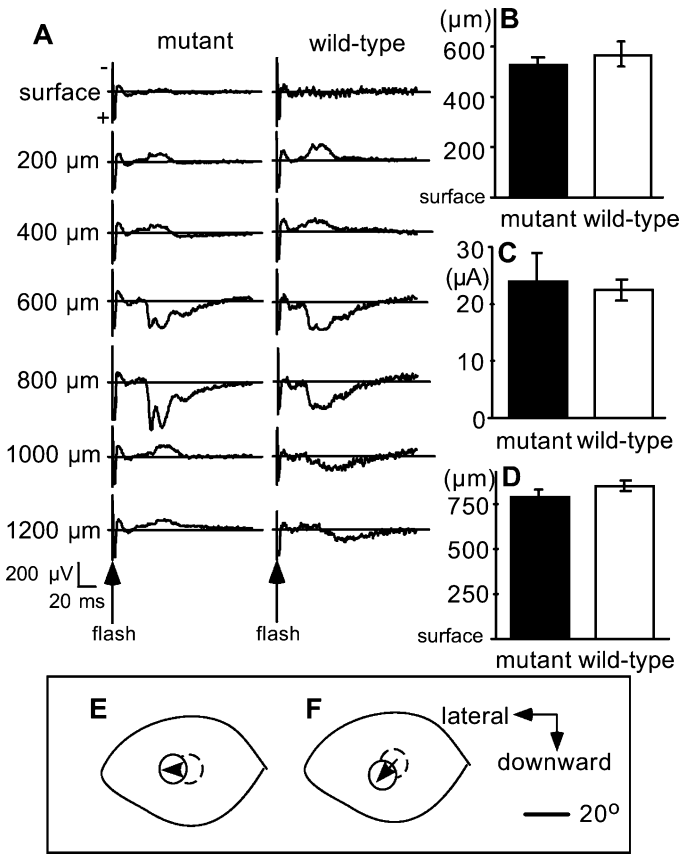

fibre inputs decreases the inhibitory outputs of Purkinje cells (e.g. Ito *et al*., 1979). We locally stimulated the paraflocculus–flocculus area with small negative train pulses via the microelectrode in alert mice, and observed stimulus-induced eye movements using the TV camera system. Local stimulation induced slow downward and/or lateral eye shifts when the electrode passed through the flocculus, as reported in rabbits (Nagao *et al*., 1985). Usually, when the electrode was placed within 0–400 μm from the surface, electrical stimulation (current strength, <50 μA) induced no eye movements, but when the electrode advanced to 600–1200 μm from the surface, stimulation induced slow eye movements in the lateral and/or downward directions (Fig. 5E and F). No difference was observed in the pattern of the evoked eye movements

FIG. 5. Comparison of electrophysiological properties of flocculus between mutant and wild-type mice. A, averaged evoked field potential for stroboscopic flashlight recorded every 200 μm from the surface of the paraflocculus under general anaesthesia. Flashlight was delivered every 4 s, and field potentials evoked to 32 flash stimulations were averaged. Although the shapes of field potentials varied between tracks, the positive-peak field potentials were recorded at 600–800 μm from the surface, where the flocculus was located. B, the mean depth at which the positive-peak field potentials were recorded in seven mutant and seven wild-type mice. We also examined the output property of the flocculus. In alert six mutant and six wild-type mice, we inserted a glass microelectrode into the paraflocculus–flocculus area and applied negative current train pulses (frequency, 300 Hz; pulse width, 0.25 ms; number of pulses, 30) at every 250 μm, and observed evoked eye movements on the TV monitor. C, the minimum threshold current intensity that induced abduction and/or downward eye movements through the electrode tract in six mutant and six wild-type mice. D, the mean depth at which the minimum threshold current intensity was recorded in each mouse. Note that the depth of minimum threshold current was observed 600–800 μm from the surface. E and F show examples of stimulation-induced eye movements observed on the monitor TV. Arrows indicate slow pupil shifts.

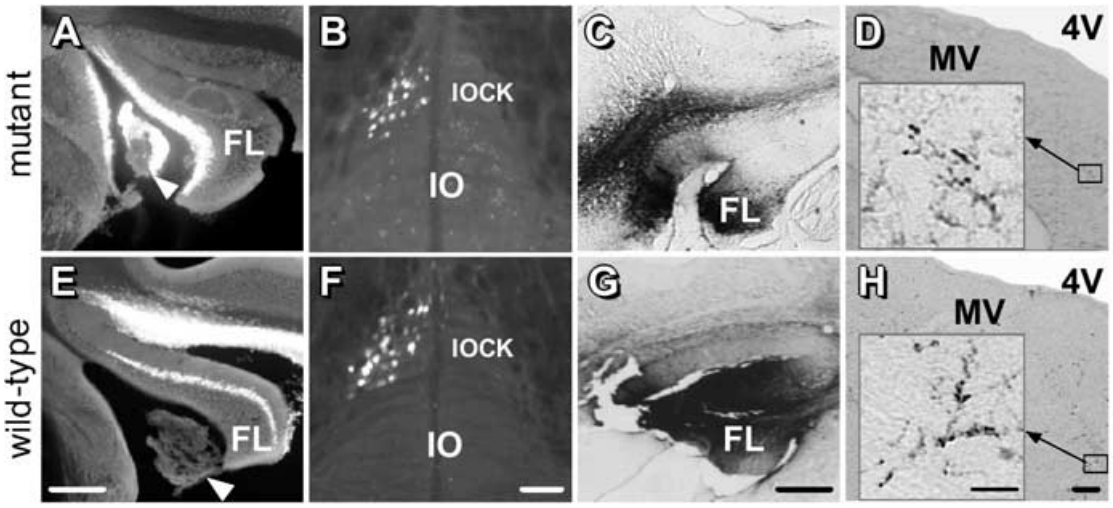

FIG. 6. Input and output connections of mutant (A–D) and wild-type (E–H) mouse cerebellar flocculi. A and E, examples of injection sites of fast blue for mutant and wild-type mice. B and F, examples of retrogradely labelled neuronal somata in the cap of Kooy of inferior olive. Twenty (B) and 24 (F) labelled somata were seen. Throughout the cap of Kooy, 106 (mutant) and 116 (wild-type) labelled neurons were seen in these cases. Labelled neurons were also seen in the beta nucleus, subnucleus of beta of medial nucleus and principal olivary nucleus, but not seen in other olivary area. C and I, injection sites of biotinylated dextran. D and H, anterogradely labelled terminals in the medial vestibular nucleus. Insets show higher magnification views marked by squares. FL, flocculus; IO, inferior olive; IOCK, inferior olive cap of Kooy; 4V, IVth ventricles; MV, medial vestibular nucleus. Arrowheads show plexus chorioideus. Scale bars, 500 μm in A, C, E and G, 200 μm in B, D, F and H, and 50 μm in insets to G and H.

or its threshold current intensity between the mutant and wild-type mice (Fig. 5C). The mean depth where minimum threshold currents were recorded during electrode tracking was 700–800 μm from the surface of the paraflocculus in both mutant and wild-type mice (Fig. 5D). Histological studies revealed that the Purkinje cell layer of the flocculus is located at this depth (data not shown).

We also examined the sources of climbing fibre inputs to the flocculus, and the location of flocculus output terminals in mutant mice. After microinjection of fast blue into the flocculus (Fig. 6A and E), retrogradely labelled somata were seen within the cap of Kooy of inferior olive in both mutant and wild-type mice (Fig. 6B and F). After injections of biotinylated dextran into the flocculus (Fig. 6C and G), anterogradely labelled terminals were seen in the medial vestibular nuclei (Fig. 6D and H) in both mutant and wild-type mice. No systematic differences were seen in the distributions of the labelled somata or terminals between mutant and wild-type mice (also see legend for Fig. 6). Thus, the climbing fibre inputs and the flocculus output organizations in PKCγ mutant mice were not greatly affected. In cases in which the injections of fast blue or biotinylated dextran spared the flocculus and covered only the paraflocculus ($n = 1$ for mutant, $n = 2$ for wild-type mice), no retrogradely labelled somata were seen in the cap of Kooy, or no labelled terminals were seen in the medial vestibular nucleus in both the mutant and wild-type mice (data not shown). The organization of the olive–flocculus–vestibular nuclei microcomplex in mice seems to be similar to those of other animal species (e.g. Ito, 1984).

Discussion

HOKR dynamics of PKCγ mutant mice

The present study revealed that the eye movements of PKCγ mutant mice were characterized by moderately depressed HOKR and normal HVOR dynamics (Fig. 1). The same tendency was noted in mice that expressed the PKC inhibitor selectively in cerebellar Purkinje cells (De Zeeuw *et al.*, 1998). The accessory visual pathway, which mediates visual signals for HOKR, is composed of the nucleus of the optic tract and nucleus reticularis tegmenti pontis (NRTP). The NRTP projects directly to the vestibular nuclear complex, and also indirectly via the cerebellar flocculus (e.g. Ito, 1984). Because the HOKR and HVOR share the final neural circuitry involving the vestibular nuclear complex and extraocular muscular motorneurons, PKCγ knockout seems to affect the HOKR gain in precerebellar optokinetic visual systems or the flocculus. Although PKCγ is abundantly expressed in the cerebellar Purkinje cells, it is not expressed in any of the accessory visual areas or retina in adult rodents (Wetsel *et al.*, 1992; Garcia & Harlan, 1997). Moreover, the visual acuity seems not to be affected in mutant mice, because gains of HOKR actually depended on the check size of the screen (Fig. 1). Thus, it is possible that the HOKR gains are depressed within the flocculus in the mutant mouse. Loss of adaptation of the HOKR to high-velocity screen oscillation that induced large retinal slips (Fig. 2) may be related to depressed HOKR gains in PKCγ mutant mice. Slight differences were noted in comparing the dynamic characteristics of ocular reflexes of PKCγ mutant mice with those of the nitric oxide synthetase (nNOS) mutant mice (Katoh *et al.*, 2000) and type-I metabotrophic glutamate receptor (mGluR1) mutant mice (Shutoh *et al.*, 2002). The HOKR gains were moderately depressed in mGluR1 mutant and PKCγ mutant mice, but not in nNOS mutant mice. The HVOR gains were not altered in PKCγ mutant or n-NOS mutant mice, but depressed stimulus-frequency dependently in the mGluR1 mutant mice. The phases of the HVOR/HOKR were not altered in PKCγ mutant or n-NOS mutant mice, but lagged in the HOKR and advanced in the HVOR in mGluR1 mutant mice.

HOKR adaptation in the PKCγ mutant mice

Sustained exposure to retinal slips for 1 h induces adaptation of HOKR in animals with no fovea. Adaptation of the HOKR was reported in the rabbit (Collewijn & Grootendorst, 1979; Nagao, 1983, 1989), mouse (Katoh *et al.*, 1998, 2000) and goldfish (Schairer & Bennett, 1986). A retinal slip velocity of >1.6–5.5°/s induced adaptation of HOKR in wild-type mice, but the mutant mice showed adaptation only to a retinal slip velocity of 2–3°/s (Fig. 2 and Table 1). The PKCγ knockout

altered retinal slip velocity dependency in the HOKR adaptation. Local application of PKC inhibitor (chelerythrine) into the flocculus had little affect on the dynamics of the HOKR, and specifically blocked adaptation of the HOKR of mutant mice to small retinal slips as well as that of wild-type mice to both small and large retinal slips (Fig. 3). Because PKC inhibitors blocked LTD (Linden & Connor, 1991, 1995; Linden *et al*., 1992; Kano *et al*., 1995), LTD seems to underlie the adaptation of the HOKR of both PKCγ mutant and wild-type mice.

Mice lacking nNOS and mGluR1 showed no HOKR adaptation (Katoh *et al*., 2000; Shutoh *et al*., 2002). Electrophysiological studies reveal the absence of LTD of parallel fibre – Purkinje cell synapses in nNOS (Lev-Ram *et al*., 1997) and mGluR1 (Aiba *et al*., 1994; Conquet *et al*., 1994) mutant mice. Adaptation of the HOKR of PKCγ mutant mice was affected but not abolished in the present study, consistent with the finding of Chen *et al*. (1995) that the LTD is not affected in PKCγ mutant mice. Thus, the parallelism between the adaptation of the HOKR and LTD is preserved in nNOS, mGluR1 and PKCγ knockout mice.

Retinal slip signals in the horizontal plane, which are necessary for the adaptation of the HOKR, seem to be transmitted to the medial part of the flocculus by climbing fibres originated from the cap of Kooy of inferior olive (e.g. Ito, 1984). Lesions of cap of Kooy of inferior olive abolished adaptation of the HOKR in mice (Katoh *et al*., 1998). Electrophysiological studies of the rabbit (Maekawa & Simpson, 1973; Miyashita & Nagao, 1984; Nagao, 1988; Kusunoki *et al*., 1990; Wylie *et al*., 1995) and monkey (Watanabe, 1985) revealed that complex spike activities recorded in the medial part of the flocculus mediate retinal slip signals that are necessary for adaptation of the HOKR. Thus, it is suggested that changes of retinal slip dependency observed in the PKCγ mutant mice may be induced by alteration of climbing fibre inputs to the flocculus. Kano *et al*. (1995) reported that mature PKCγ mutant mice have persistent multiple climbing fibre innervations of Purkinje cells. The climbing fibre responsiveness may be affected if the floccular Purkinje cells of PKCγ mutant mice also receive climbing fibres from inferior olivary neurons outside the cap of Kooy. However, the present study failed to reveal differences in flash-evoked visual climbing fibre field responses (Fig. 5), locations of climbing fibre input sources between the mutant and wild-type mice (Fig. 6) or outputs of floccular Purkinje cells (Figs 5 and 6). Quantitative evaluations of complex spike retinal slip responsiveness at single-unit level may be necessary to determine whether climbing fibre multiple innervations of Purkinje cells actually underlie the altered retinal slip dependency in PKCγ mutant mice. Impaired climbing fibre synapse elimination of Purkinje cells was also seen in mGluR1 mutant mice (Kano *et al*., 1997), but not in n-NOS mutant mice (see Shutoh *et al*., 2002).

Role of PKC subtypes in HOKR adaptation

Although PKCγ is abundantly expressed in the Purkinje cells, adaptation of the HOKR and also LTD (Chen *et al*., 1995) were preserved in PKCγ mutant mice. Moreover, the present study revealed that application of the PKC inhibitor (chelerythrine) blocked the HOKR adaptation of PKCγ mutant mice. An electrophysiological study revealed that intracellular applications of an inhibitory peptide of PKC completely abolished LTD in slices obtained from wild-type mice, and markedly depressed LTD in slices obtained from PKCγ mutant mice (Chen *et al*., 1995). On the other hand, LTD was abolished in slices obtained from transgenic mice that expressed a non-specific inhibitor of PKC subtypes (De Zeeuw *et al*., 1998). Taken together with the results from these studies, we suggest that other PKC subtypes, rather than the PKCγ, may play a key role in the adaptation of HOKR and also in LTD. Our histological study revealed that among the subtypes of the Ca^{2+}-dependent PKC family, α and γ are both expressed, and β_1 or β_2 are not detected in the flocculus Purkinje cells (Fig. 4). Thus, we suggest that PKCα may be a candidate that plays a crucial role in the HOKR adaptation and also in LTD. Hirono *et al*. (2001) also suggest that PKCα and/or β_1, and not PKCγ, may be involved in the induction of LTD in the vermis. It is also reported that PKCδ, a Ca^{2+}-independent isoform of PKC, was abundantly expressed in the rat flocculus (Chen & Hillman, 1993; Merchenthaler *et al*., 1993). A possibility still remains that chelerythrine blocks adaptation of the HOKR through its blocking action on PKCδ. Subtype-specific PKC blockers are necessary to determine whether PKCα actually plays a crucial role in the adaptation of the HOKR and/or LTD.

The present study indicates that PKCγ may play a role in determining the retinal slip dependency in the HOKR adaptation. Two possible mechanisms are suggested to explain why PKCγ plays such a role in HOKR adaptation. One mechanism involves subtle neuronal circuitry developmental defects caused by PKCγ knockout, i.e. impaired elimination of multiple climbing fibre innervations of Purkinje cells, which has been referred to previously (Kano *et al*., 1995). Another possibility is that PKCγ may interact with the intracellular LTD mechanism. Strong depolarization of Purkinje cells by climbing fibre inputs induced Ca^{2+} influx through voltage-gated Ca^{2+} channels. Because PKCγ mutation did not affect the functioning of these voltage-gated Ca^{2+} channels (Kano *et al*., 1995), small retinal slip signals may induce a small Ca^{2+} increase, and large retinal slips a relatively large Ca^{2+} increase in flocculus Purkinje cells of PKCγ mutant mice. If PKCα plays a major role in LTD, it may bind Ca^{2+} and phosphorylate α-amino-3-hydroxy-5-methylisoxazole-4-propionic acid (AMPA) receptors (Nakazawa *et al*., 1995) to trigger their internalization (Xia *et al*., 2000). We cannot exclude the possibility that the PKCγ may affect LTD when intracellular Ca^{2+} concentration is relatively high. In any case, the PKC subtypes, located near the synaptic terminals of Purkinje cell dendrite spines (Cardell *et al*., 1998), may somehow play different roles in the LTD and adaptation of the HOKR. A difference in roles for Ca^{2+}-dependent PKC subtypes in flocculo-nodular Purkinje cells was suggested in the early compensatory phase after a unilateral peripheral vestibular lesion in the rat (Goto *et al*., 1997; Balaban *et al*., 1999). How the PKCγ may mediate such a unique role in the HOKR adaptation should be examined in future experiments.

Acknowledgements

We are extremely grateful to Dr M. Ito (RIKEN, BSI) for reading the manuscript. We also wish to thank Dr M. Yamakado (Jichi Medical Sch.) for his technical advice on histology.

Abbreviations

AMPA, α-amino-3-hydroxy-5-methylisoxazole-4-propionic acid; BD, biotinylated dextran; FB, fast blue; HOKR, horizontal optokinetic response; HVOR, horizontal vestibulo-ocular reflex; LTD, long-term depression; mGluR, metabotropic glutamate receptor; nNOS, neural nitric oxide synthase; NRTP, nucleus reticularis tegmenti pontis; PKC, protein kinase C.

References

Abeliovich, A., Chen, C., Goda, Y., Silva, A.J., Stevens, C.F. & Tonegawa, S. (1993) Modified hippocampal long-term potentiation in PKCγ-mutant mice. *Cell*, **75**, 1253–1262.

Aiba, A., Kano, M., Chen, C., Stanton, M.E., Fox, G.D., Herrup, K., Zwingman, T.A. & Tonegawa, S. (1994) Deficient cerebellar long-term depression and impaired motor learning in mGluR1 mutant mice. *Cell*, **79**, 377–388.

Balaban, C.D., Freilino, M. & Romero, G.G. (1999) Protein kinase C inhibition blocks the early appearance of vestibular compensation. *Brain Res.*, **845**, 97–101.

Cardell, M., Landsend, A.S., Eidet, J., Wieloch, T., Blackstad, T.W. & Ottersen, O.P. (1998) High resolution immunogold analyses reveals distinct subcellular

compartmentation of protein kinase Cγ and δ in rat Purkinje cells. *Neuroscience*, **82**, 709–725.
Chen, S. & Hillman, D.E. (1993) Compartmentation of the cerebellar cortex by protein kinase Cδ. *Neuroscience*, **56**, 177–188.
Chen, C., Kano, M., Abeliovich, A., Chen, L., Bao, S., Kim, J.J., Hashimoto, K., Tompson, R.F. & Tonegawa, S. (1995) Impaired motor coordination correlates with persistent multiple climbing fiber innervation in PKCγ mutant mice. *Cell*, **83**, 1233–1242.
Chen, C. & Tonegawa, S. (1977) Molecular genetic analysis of synaptic plasticity, activity-dependent neural development, learning and memory in mammalian brain. *Annu. Rev. Neurosci.*, **20**, 157–184.
Collewijn, H. & Grootendorst, A.F. (1979) Adaptation of optokinetic and vestibulo-ocular reflexes to modified visual input in the rabbit. *Prog. Brain Res.*, **50**, 771–781.
Conquet, F., Bashir, Z.I., Davies, C.H., Daniel, H., Ferraguti, F., Bordi, F., Franz-Bacon, K., Reggiani, A., Matarese, V., Conde, F., Collingridge, G.L. & Crépel, F. (1994) Motor deficit and impairment of synaptic plasticity in mice lacking mGluR1. *Nature*, **372**, 237–243.
Crépel, F. & Krupa, M. (1988) Activation of protein kinase C induces a long-term depression of glutamate sensitivity of cerebellar Purkinje cells. An in vitro study. *Brain Res.*, **458**, 397–401.
Daniel, H., Levenes, C. & Crépel, F. (1998) Cellular mechanisms of cerebellar LTD. *Trends Neurosci.*, **21**, 401–407.
De Zeeuw, C.I., Hansel, C., Bian, F., Koekkoek, S.K.E., van Alphen, A.M., Linden, D.J. & Oberdick, J. (1998) Expression of a protein kinase C inhibitor in Purkinje cells blocks cerebellar LTD and adaptation of the vestibulo-ocular reflex. *Neuron*, **20**, 495–508.
Franklin, K.B.J. & Paxinos, G. (1997) *The Mouse Brain in Stereotaxic Coordinates.* Academic Press, San Diego.
Garcia, M.M. & Harlan, R.E. (1997) Protein kinase C in central vestibular, cerebellar, and precerebellar pathways of the rat. *J. Comp. Neurol.*, **385**, 26–42.
Goossens, J., Daniel, H., Rancillac, A., van der Steen, J., Oberdick, J., Crépel, F., De Zeeuw, C.I. & Frens, M.A. (2001) Expression of protein kinase C inhibitor blocks cerebellar long-term depression without affecting Purkinje cell excitability in alert mice. *J. Neurosci.*, **21**, 5813–5823.
Goto, M.M., Romero, G.G. & Balaban, C.D. (1997) Transient changes in flocculonodular lobe protein kinase C expression during vestibular compensation. *J. Neurosci.*, **17**, 4367–4381.
Herbert, J.M., Augereau, J.M., Gleye, J. & Maffrand, J.P. (1990) Chelerythrine is a potent and specific inhibitor of protein kinase C. *Biochem. Biophys. Res. Commun.*, **172**, 993–999.
Hidaka, H., Tanaka, T., Onoda, K., Hagiwara, M., Watanabe, M., Ohta, H., Ito, Y., Tsurudome, M. & Yoshida, T. (1988) Cell type-specific expression of protein kinase C isozymes in the rabbit cerebellum. *J. Biol. Chem.*, **263**, 4523–4526.
Hirono, M., Sugiyama, T., Kishimoto, Y., Sakai, I., Miyazawa, T., Kishio, M., Inoue, H., Nakao, K., Ikeda, M., Kawahara, S., Kirino, Y., Katsuki, M., Horie, H., Ishikawa, Y. & Yoshioka, T. (2001) Phospholipase Cβ4 and protein kinase Cα and/or protein kinase CβI are involved in the induction of long term depression in cerebellar Purkinje cells. *J. Biol. Chem.*, **30**, 45236–45242.
Ito, M. (1984) *The Cerebellum and Neural Control.* Raven Press, New York.
Ito, M. (1989) Long-term depression. *Annu. Rev. Neurosci.*, **12**, 85–102.
Ito, M. (2001) Cerebellar long-term depression: characterization, signal transduction, and functional roles. *Physiol. Rev.*, **81**, 1143–1195.
Ito, M., Nisimaru, N. & Shibuki, K. (1979) Destruction of inferior olive induces rapid depression in synaptic action of cerebellar Purkinje cells. *Nature*, **277**, 568–569.
Jastreboff, P.J. (1979) Evaluation and statistical judgment of neural responses to sinusoidal stimulation in cases with superimposed drift and noise. *Biol. Cybern.*, **33**, 113–120.
Kano, M., Hashimoto, K., Chen, C., Abeliovich, H., Aiba, A., Kurihara, H., Watanabe, M., Inoue, Y. & Tonegawa, S. (1995) Impaired synapse elimination during cerebellar development in PKCγ mutant mice. *Cell*, **83**, 1223–1231.
Kano, M., Hashimoto, K., Kurihara, H., Watanabe, M., Inoue, Y., Aiba, A. & Tonegawa, S. (1997) Persistent multiple climbing fiber innervation of cerebellar Purkinje cells in mice lacking mGluR1. *Neuron*, **18**, 71–79.
Katoh, A., Kitazawa, H., Itohara, S. & Nagao, S. (1998) Dynamic characteristics and adaptability of mouse vestibulo-ocular and optokinetic response eye movements and the role of the flocculo-olivary system revealed by chemical lesions. *Proc. Natl Acad. Sci. USA*, **95**, 7705–7710.
Katoh, A., Kitazawa, H., Itohara, S. & Nagao, S. (2000) Inhibition of nitric oxide synthesis and gene knockout of neuronal nitric oxide synthase impaired adaptation of mouse optokinetic response eye movements. *Learn. Mem.*, **7**, 220–226.
Kusunoki, M., Kano, M., Kano, M.-S. & Maekawa, K. (1990) Nature of optokinetic response and zonal organization of climbing fiber afferents in the vestibulocerebellum of the pigmented rabbit. I. The flocculus. *Exp. Brain Res.*, **81**, 225–237.
Lev-Ram, V., Nebyelul, Z., Ellisman, M.H., Huang, P.L. & Tsien, R.Y. (1997) Absence of cerebellar long-term depression in mice lacking neuronal nitric oxide synthase. *Learn. Mem.*, **4**, 169–177.
Linden, D.J. & Connor, J.A. (1995) Long-term synaptic depression. *Annu. Rev. Neurosci.*, **18**, 319–357.
Linden, D.J. & Connor, J.A. (1991) Participation of postsynaptic PKC in cerebellar long-term depression in culture. *Science*, **254**, 1656–1659.
Linden, D.J., Smeyne, M., Sun, S.C. & Connor, J.A. (1992) An electrophysiological correlate of protein kinase C isozyme distribution in cultured cerebellar neurons. *J. Neurosci.*, **12**, 3601–3608.
Maekawa, K. & Simpson, J.I. (1973) Climbing fiber responses evoked in vestibulocerebellum of rabbit from visual system. *J. Neurophysiol.*, **36**, 649–666.
Merchenthaler, I., Liposits, Z., Reid, J.J. & Wetsel, W.C. (1993) Light and electron microscopic immunohistochemical localization of PKCδ immunoreactivity in the rat central nervous system. *J. Comp. Neurol.*, **336**, 378–399.
Miyashita, Y. & Nagao, S. (1984) Analysis of signal content of Purkinje cell responses to optokinetic stimuli in the rabbit cerebellar flocculus by selective lesions of brain stem pathway. *Neurosci. Res.*, **1**, 223–241.
Nagao, S. (1983) Effects of vestibulocerebellar lesions upon dynamic characteristics and adaptation of vestibulo-ocular and optokinetic eye movements in pigmented rabbits. *Exp. Brain Res.*, **53**, 36–46.
Nagao, S. (1988) Behavior of floccular Purkinje cells correlated with adaptation of horizontal optokinetic eye movement response in pigmented rabbits. *Exp. Brain Res.*, **73**, 489–497.
Nagao, S. (1989) Role of cerebellar flocculus in adaptive interaction between optokinetic eye movement response and vestibulo-ocular reflex in pigmented rabbits. *Exp. Brain. Res.*, **77**, 541–551.
Nagao, S. (1990) A non-invasive method for real-time eye position recording with an infrared TV-camera. *Neurosci. Res.*, **8**, 210–213.
Nagao, S., Ito, M. & Karachot, L. (1985) Eye fields in the cerebellar flocculus of pigmented rabbits determined with local electrical stimulation. *Neurosci. Res.*, **3**, 39–51.
Nakazawa, K., Mikawa, S., Hashikawa, T. & Ito, M. (1995) Transient and persistent phosphorylation of AMPA-type glutamate receptor subunits in cerebellar Purkinje cells. *Neuron*, **15**, 697–709.
Nishizuka, Y. (1988) The molecular heterogeneity of protein kinase C and its implications for cellular regulation. *Nature*, **334**, 661–665.
Nishizuka, Y. (1992) Signal transduction: crosstalk. *Trends Biochem. Sci.*, **17**, 367–443.
Schairer, J.O. & Bennett, M.V. (1986) Changes in gain of the vestibulo-ocular reflex induced by sinusoidal visual stimulation in goldfish. *Brain Res.*, **373**, 177–181.
Shinomura, T., Asaoka, Y., Oka, M., Yoshida, K. & Nishizuka, Y. (1991) Synergisticaction of diacylglycerol and unsaturated fatty acid for protein kinase C activation: its possible implications. *Proc. Natl Acad. Sci. USA*, **88**, 5149–5153.
Shutoh, F., Katoh, A., Kitazawa, H., Aiba, A., Itohara, S. & Nagao, S. (2002) Loss of adaptability of horizontal optokinetic response eye movements in mGluR1 knockout mice. *Neurosci. Res.*, **42**, 141–145.
Shutoh, F., Katoh, A., Kitazawa, H., Ohki, M., Itohara, S. & Nagao, S. (2001) Neural mechanisms underlying the abnormal characteristics of eye movements seen in mice devoid of protein C-γ subunit. *Neurosci. Res.*, **25** (Suppl.), S120.
Stahl, J.S., van Alphen, A.M. & De Zeeuw, C.I. (2000) A comparison of video and magnetic search coil recording of mouse eye movements. *J. Neurosci. Meth.*, **99**, 101–110.
Tanaka, C. & Nishizuka, Y. (1994) The protein kinase C family for neuronal signaling. *Annu. Rev. Neurosci.*, **17**, 551–567.
Watanabe, E. (1985) Role of the primate flocculus in adaptation of the vestibulo-ocular reflex. *Neurosci. Res.*, **3**, 20–38.
Wetsel, W.C., Khan, W.A., Merchenthaler, I., Rivera, H., Halpern, A.E., Phung, H.M., Negro-Vilar, A. & Hannun, Y.A. (1992) Tissue and cellular distribution of the extended family of protein kinase C isozymes. *J. Cell Biol.*, **117**, 121–133.
Wylie, D.R., De Zeeuw, C.I. & Simpson, J.I. (1995) Temporal relations of the complex spike activity of Purkinje cell pairs in the vestibulocerebellum of rabbits. *J. Neurosci.*, **15**, 2875–2887.
Xia, J., Chung, H.J., Wihler, C., Huganir, R.L. & Linden, D.J. (2000) Cerebellar long-term depression requires PKC-regulated interactions between GluR2/3 and PDZ domain-containing proteins. *Neuron*, **28**, 499–510.